CHAPTER 5 *Applications to problems with numerically simulated response*

5.1 Introduction

Design optimization uses numerical models to simulate the behaviour of engineering systems. These simulation models are often computationally expensive because they involve numerical tools such as the finite element method. Instead, approximations can be constructed from a set of computer experiments using the original numerical model of the system (numerical simulation).

In this chapter, the genetic programming methodology is applied with two purposes. In the first three examples, different aspects of the approximation model building are studied based on simulated data from models known in advance. The fourth example deals with the damage recognition in steel structures based on the approximation of a response obtained by a finite element model.

5.2 Role of the number of experiments

Generally, a large number of points in the plan of experiments is desirable in order to provide more information to the genetic programming algorithm. To illustrate these aspects, the following expression has been tested:

$$\left(30 + x_1 \sin(x_1)\right) \left(4 + \mathrm{e}^{-x_2}\right) \tag{5.1}$$

Two tests were performed with data generated with a plan of experiments of 10 points (Figure 5.1) and 20 points (Figure 5.2). The sine and exponential functions were included in the functional set. Results show that the higher the number of experiments, the better the approximation. A history of runs is presented in Figure 5.3.

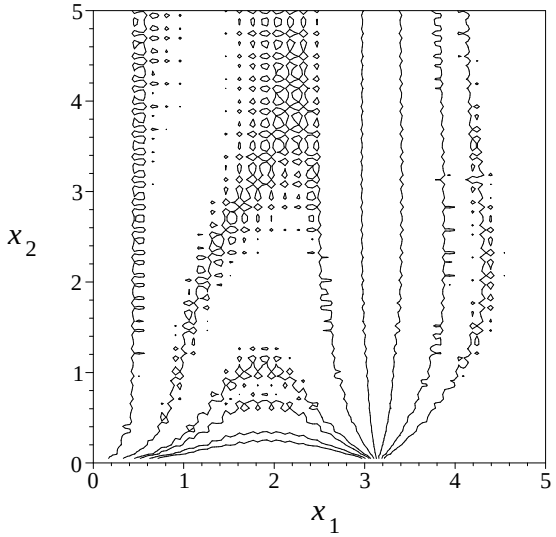

Figure 5.1 Approximation with 10 point plan of experiments

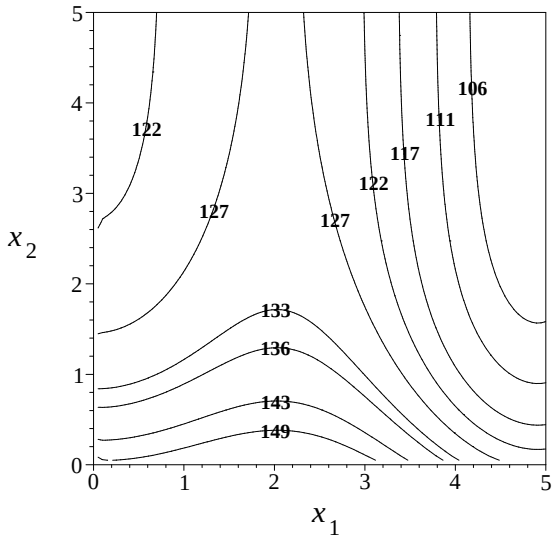

Figure 5.2 Approximation with 20 point plan of experiments (same as original)

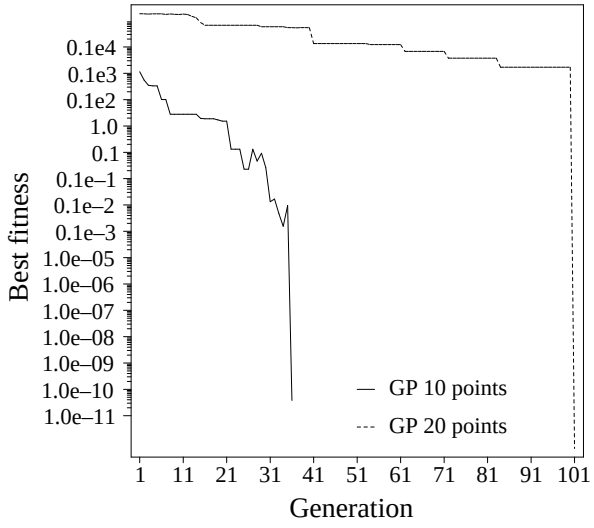

Figure 5.3 History of runs (best fitness as defined in (4.4))

5.3 Three-bar truss

Functions in the three-bar truss optimization problem described in Haftka and Gurdal (1993) have been approximated. The two design variables x_1 and x_2 describe the cross-sectional areas of individual bars (Figure 5.4), the objective function is the volume of the material and the constraints limit the stresses in all bars and the displacement of the free node. The set of response data was generated using the plan of experiments (3.8), which was then used to build the global approximations of the objective function and the constraints.

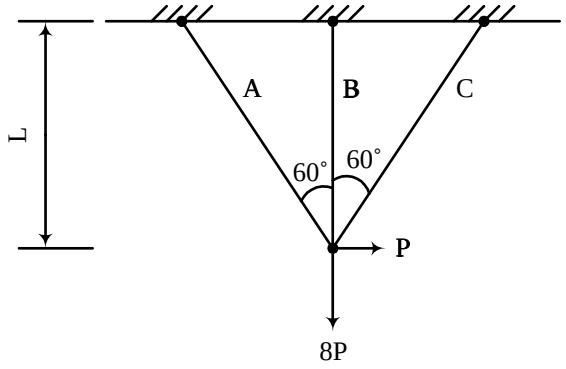

$x_1 = A_A = A_C$

$x_2 = A_B$

$E = 200\ KN/mm^2$

$P = 10\ KN$

$L = 1000\ mm$

Figure 5.4 Three-bar truss approximation problem

The output of the algorithm still needs some manual post-processing in order to get rid of those terms in the expression that give a null or tiny contribution, for example when the same value is added and subtracted. It can be suggested to run the problem several times in order to identify, by comparison, the most likely components. The optimization problem is reduced to the approximated one shown in Table 5.1.

Table 5.1 Results of three-bar truss function approximation

Original Functions	Approximations
$F_0 = 1000 * (4 * x_1 + x_2) \rightarrow min$	$\tilde{F}_0 = 4000 * x_1 + 1000 * x_2 \rightarrow min$
Subject to:	
$F_1 = \frac{400}{0.25 * x_1 + x_2} \leq 1$	$\tilde{F}_1 = \frac{106373.40}{66.48 * x_1 + 265.94 * x_2} \leq 1$
$F_2 = 25 * \left(\frac{(0.25 * \sqrt{3} + 6) * x_1 + \sqrt{3} * x_2}{3 * x_1 * x_2 + 0.75 * x_1^2} \right) \leq 1$	$\tilde{F}_2 = \frac{-17292.79 * x_1 - 4655.76 * x_2}{-(322.56 * x_2 + 80.65 * x_1) * x_1} \leq 1$
$F_3 = \frac{200}{0.25 * x_1 + x_2} \leq 1$	$\tilde{F}_3 = \frac{-41886.67}{-52.35 * x_1 - 209.41 * x_2} \leq 1$
$F_4 = 25 * \left(\frac{(-0.25 * \sqrt{3} + 6) * x_1 - \sqrt{3} * x_2}{3 * x_1 * x_2 + 0.75 * x_1^2} \right) \leq 1$	$\tilde{F}_4 = \frac{8170.86 * x_1 - 2542.18 * x_2}{(176.12 * x_2 + 44.03 * x_1) * x_1} \leq 1$

5.4 Rosenbrock's function and the use of sensitivity information

Rosenbrock's valley function is a classic optimization problem. The significance of this function is that it has "banana-shaped" contours, making it difficult for nonlinear programming algorithms. The global optimum is inside a long, curved and narrow valley. The function is defined as follows:

$$F(x_1, x_2) = 100 * \left(x_2 - x_1^2 \right)^2 + (1 - x_1)^2 \tag{5.2}$$

Figure 5.5 shows the contour plot and the surface plot of expression (5.2).

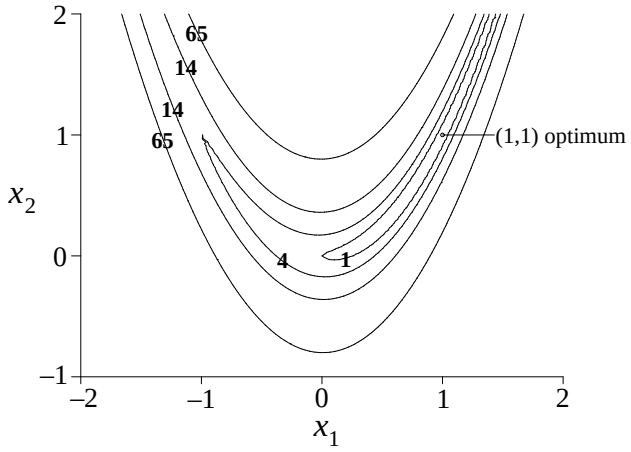

(a) Contour plot

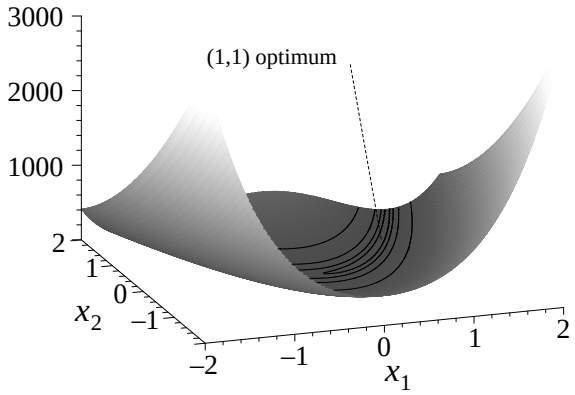

(b) Surface plot

Figure 5.5 Rosenbrock's function

With a population of 200 individuals, the approximation of Rosenbrock's function has been tested with and without the use of sensitivity information.

5.4.1 Approximation without sensitivity information

GP has been run with a plan of experiments of 5 and 10 points. In the case of 5 points, a solution with good fitness has been evolved, but leading to a completely different model as compared to (5.2).

$$F(x_1, x_2) = -11433.909897 - 7272.990034 * \sqrt{(x_1)} / x_2 + 7300.037743 * x_2 + 3847.116717 * x_1^2 - 3829.663346 * x_2 * x_1 \quad (5.3)$$

The reason for this difference is that insufficient information was passed to GP to represent an accurate solution. When approximated with 10 points, the solution was identical to function (5.2).

5.4.2 Approximation with sensitivity information

When first order derivatives, as defined in (3.3), were included in the approximation of Rosenbrock's function with a plan of experiments of 5 points, the algorithm exactly matched the original expression (5.2). This suggests that, if available, derivatives provide with more information, thus improving the convergence characteristics. If the derivatives are not available, the inclusion of more points in the plan of experiments will be necessary. Figure 5.6 shows a history of the runs where the vertical axis is in logarithmic scale.

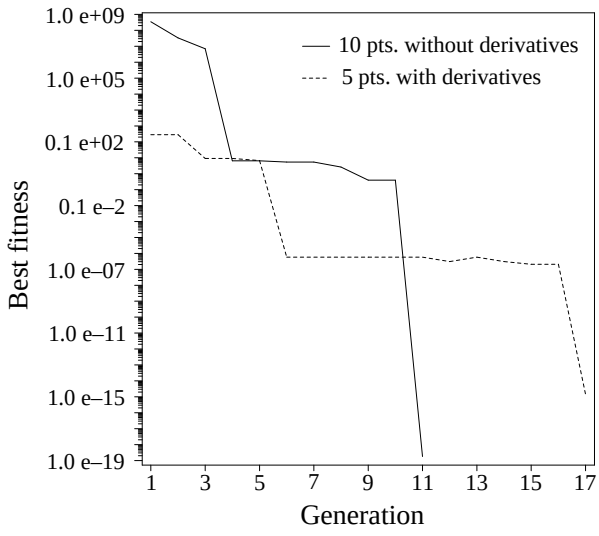

Figure 5.6 History of runs for Rosenbrock's function

5.5 Recognition of damage in steel structures

5.5.1 Introduction

Visual inspection and field testing are usually employed to identify the location and degree of damage of an engineering structure. However, this can be expensive and time consuming. Alternatively, changes in the dynamic structural characteristics provide a non-destructive method of testing. In this application, natural frequencies have been obtained by measurements at a number of points of the structure (Ravaii et al., 1998). These characteristics can be used to calculate a local decrease in the stiffness of the structure that indicates the presence of structural damage.

The damage recognition problem has been formulated as an optimization problem and solved using the response surface methodology. The analytical expressions, representing response surfaces, have been built using the genetic programming methodology in order to obtain high quality approximations. The advantage of this approach is that the resulting optimization problem is simple and, therefore, does not require extensive computations as compared to a finite element analysis.

5.5.2 Identification problem formulation

In the finite element formulation, the presence of damage is defined in terms of the stiffness and mass matrix because variations in these matrices result in changes of the frequency response. The optimization variables $\boldsymbol{x}$ have been introduced such as

sectional properties or material parameters. An individual variable x_i describes the extent of possible damage at *i*-th location.

The damage identification problem can be formulated as follows (Ravaii et al., 1998): find the values of the optimization variables $\boldsymbol{x}$ by minimizing the differences between the frequencies ω_i^m measured in the course of laboratory experiment or operation and the frequencies $\omega_i^a(\boldsymbol{x})$ obtained by the finite element analysis:

$$F(\boldsymbol{x}) = \sum_{i=1}^{M} w_i \left(\frac{\omega_i^m - \omega_i^a(\boldsymbol{x})}{\omega_i^m} \right)^2 \rightarrow \min$$
$$A_j \le x_j \le B_j, \quad j = 1,\ldots,N \tag{5.4}$$

where M is the total number of modes of vibration used for the identification, A_i and B_i are appropriate lower and upper bounds on the optimization variables and the weights w_i describe the relative importance of the match between the frequencies of the *i*-th mode.

According to the response surface methodology, the original optimization problem (5.4) is replaced by a simpler mathematical programming problem

$$\tilde{F}(\boldsymbol{x}) \rightarrow \min, \quad A_j \le x_j \le B_j, \quad j = 1,\ldots,N \tag{5.5}$$

The function $\tilde{F}(\boldsymbol{x})$ presents a global approximation of the corresponding original function $F(\boldsymbol{x})$ in (5.4) and the solution of the problem (5.5) is considered as an approximation of the solution of the problem (5.4).

Alternatively, each of the individual frequencies $\omega_i^a(\boldsymbol{x}), i = 1,...M$ in (5.4) can be approximated by simpler expressions $\tilde{\omega}_i^a(\boldsymbol{x})$ and the objective function $\tilde{F}(\boldsymbol{x})$ can be assembled similarly to (5.4) using the approximated frequencies:

$$\begin{aligned} \tilde{F}(\boldsymbol{x}) &= \sum_{i=1}^{M} w_i \left(\frac{\omega_i^m - \tilde{\omega}_i^a(\boldsymbol{x})}{\omega_i^m} \right)^2 \rightarrow \min \\ A_j &\le x_j \le B_j, \quad j = 1,..., N \end{aligned} \tag{5.6}$$

The advantage of the formulation (5.6) is that the approximations $\tilde{\omega}_i^a(\boldsymbol{x})$ can be built once and then used many times for damage detection in a new structure of the same geometry using new sets of the experimental data $\omega_i^m(\boldsymbol{x}), i = 1,...M$.

5.5.3 Experimental results

The test structure used in the investigation (Ravaii et al., 1998) was a steel portal frame as shown in Figure 5.7. The damage was applied at the location close to the apex, reducing the cross section area to 54% of the original value for the undamaged structure.

For the finite element model, Ravaii et al. (1998) assumed that damage could only occur at a joint. Because of the symmetry, the optimization problem is reduced to three variables, one at the apex, next to the corner and at the base (Figure 5.7). In order to determine the smallest number of modes necessary to use to reliably detect the damage, the number of modes was incremented one by one and found to be four, as reported by Ravaii et al. (1998).

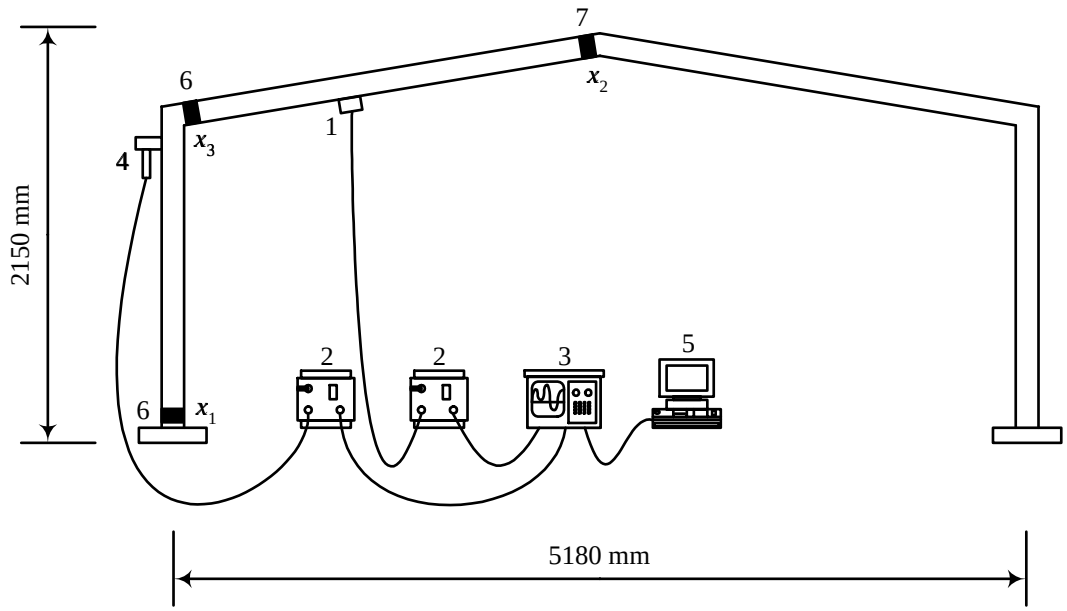

1. Accelerometer
2. Charge amplifier
3. Dual channel analyser
4. Instrumented hammer
5. Personal computer
6. Possible damage positions
7. Actual damage position

Figure 5.7 Experimental setup

5.5.4 Results of damage recognition

In the formulation of the optimization problem (5.4) the number of optimization variables $N = 3$, the number of used frequencies $M = 4$, and x_1, x_2, x_3 describe the percentage of reduction of cross-sectional area in three locations as shown in Figure 5.7. The description of actual damage corresponds to the following set of optimization variables: $x_1 = 100$, $x_2 = 54$, $x_3 = 100$, i.e. damage in second location.

The approximation procedure using GP has been carried out following two different approaches as described in section 5.5.2: approximation of the original

optimization problem (5.4), as defined in (5.5), and approximation of the individual frequencies corresponding to the first four modes of vibration, as defined in (5.6).

For the 3-dimensional graphical representation, the approximation functions have been plotted fixing one of the three optimization variables, corresponding to possible damage locations, i.e. $x_1 = 100$, $x_2 = 54$, $x_3 = 100$.

Figure 5.8 shows the original function (5.4) and the overall approximation functions as defined by expression (5.5) using the values of the function (5.4) at $P = 20$ and $P = 50$ points of the optimization variable space.

The solution of the simplified optimization problem (5.5) has been obtained in two steps of approximation building. In the first step the following values of lower and upper bounds have been selected: $A_j = 10$ and $B_j = 110$, $j = 1, 2, 3$. In the second step the size of the search domain of the optimization variable space, defined by A_j and B_j, has been reduced by half and the new approximations have been constructed. When the approximation have been built using 20 points, the following solution has been obtained: $x_1 = 72.50$, $x_2 = 50.80$, $x_3 = 110.0$. Using 50 points, the following solution has been obtained: $x_1 = 96.61$, $x_2 = 49.51$, $x_3 = 106.63$ (Table 5.2).

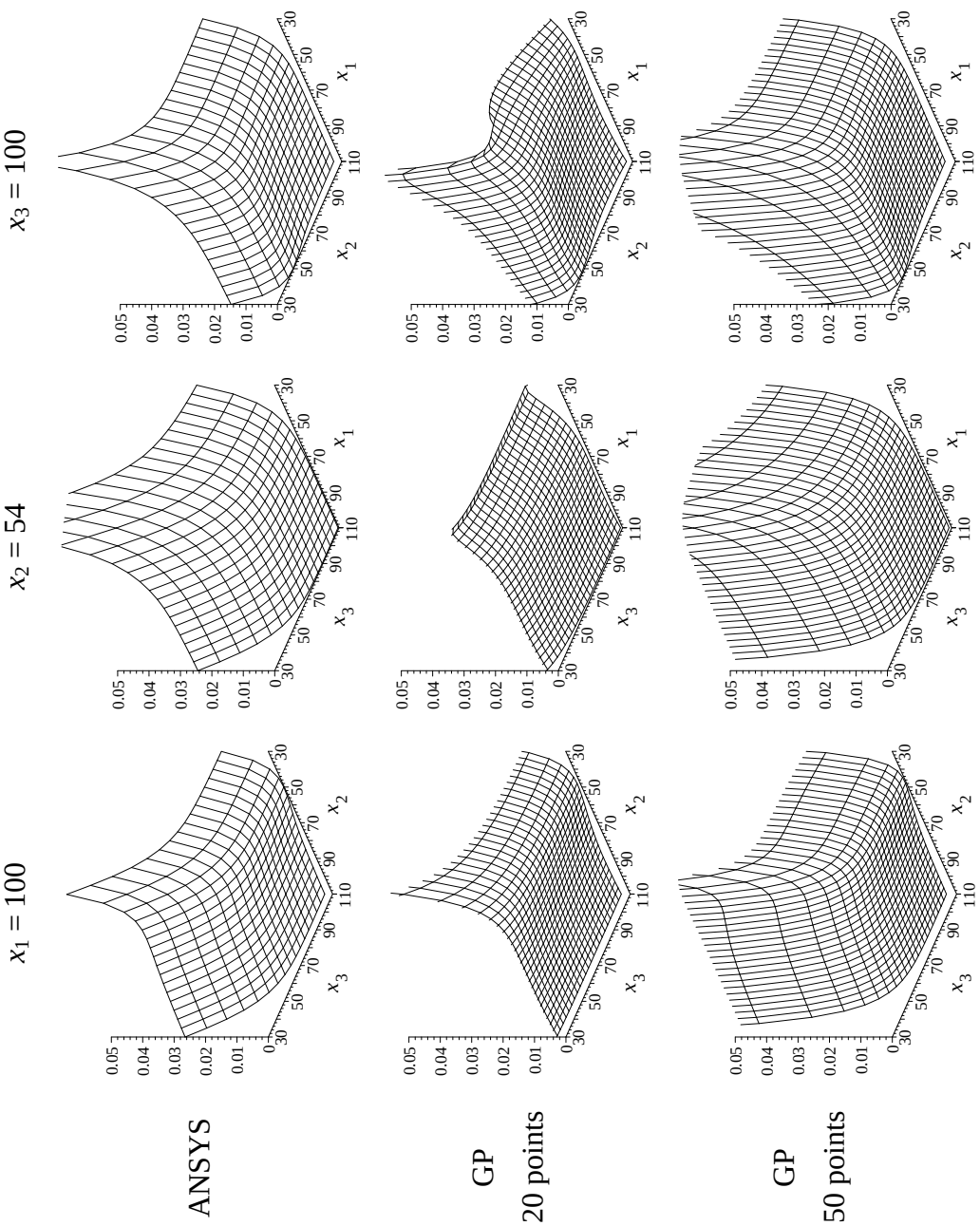

Figure 5.8 Approximation of the overall expression

Table 5.2 History of the approximation

	Iteration	Move limits	Optimum
GP 20 points	1	$10.0 \le x_1 \le 110.0$	$x_1 = 69.97$
		$10.0 \le x_2 \le 110.0$	$x_2 = 61.11$
		$10.0 \le x_3 \le 110.0$	$x_3 = 110.0$
	2	$44.96 \le x_1 \le 94.96$	$x_1 = 72.50$
		$36.11 \le x_2 \le 86.11$	$x_2 = 50.80$
		$85.0 \le x_3 \le 110.0$	$x_3 = 110.0$
GP 50 points	1	$10.0 \le x_1 \le 110.0$	$x_1 = 71.61$
		$10.0 \le x_2 \le 110.0$	$x_2 = 74.50$
		$10.0 \le x_3 \le 110.0$	$x_3 = 85.40$
	2	$46.61 \le x_1 \le 96.61$	$x_1 = 96.61$
		$49.51 \le x_2 \le 99.51$	$x_2 = 49.51$
		$60.39 \le x_3 \le 110.0$	$x_3 = 106.63$

When the approximation functions were obtained as a combination of approximations for the individual frequencies, as defined by the expression (5.6), the following solutions have been obtained in one step: $x_1 = 79.7$, $x_2 = 51.1$, $x_3 = 89.6$ using 20 points and $x_1 = 92.6$, $x_2 = 50.1$, $x_3 = 110.0$ using 50 points. Figure 5.9 shows the approximation of individual frequencies for $x_1 = 100$, Figure 5.10 for $x_2 = 54$ and Figure 5.11 for $x_3 = 100$. Figure 5.12 shows the final expression as defined in (5.6).

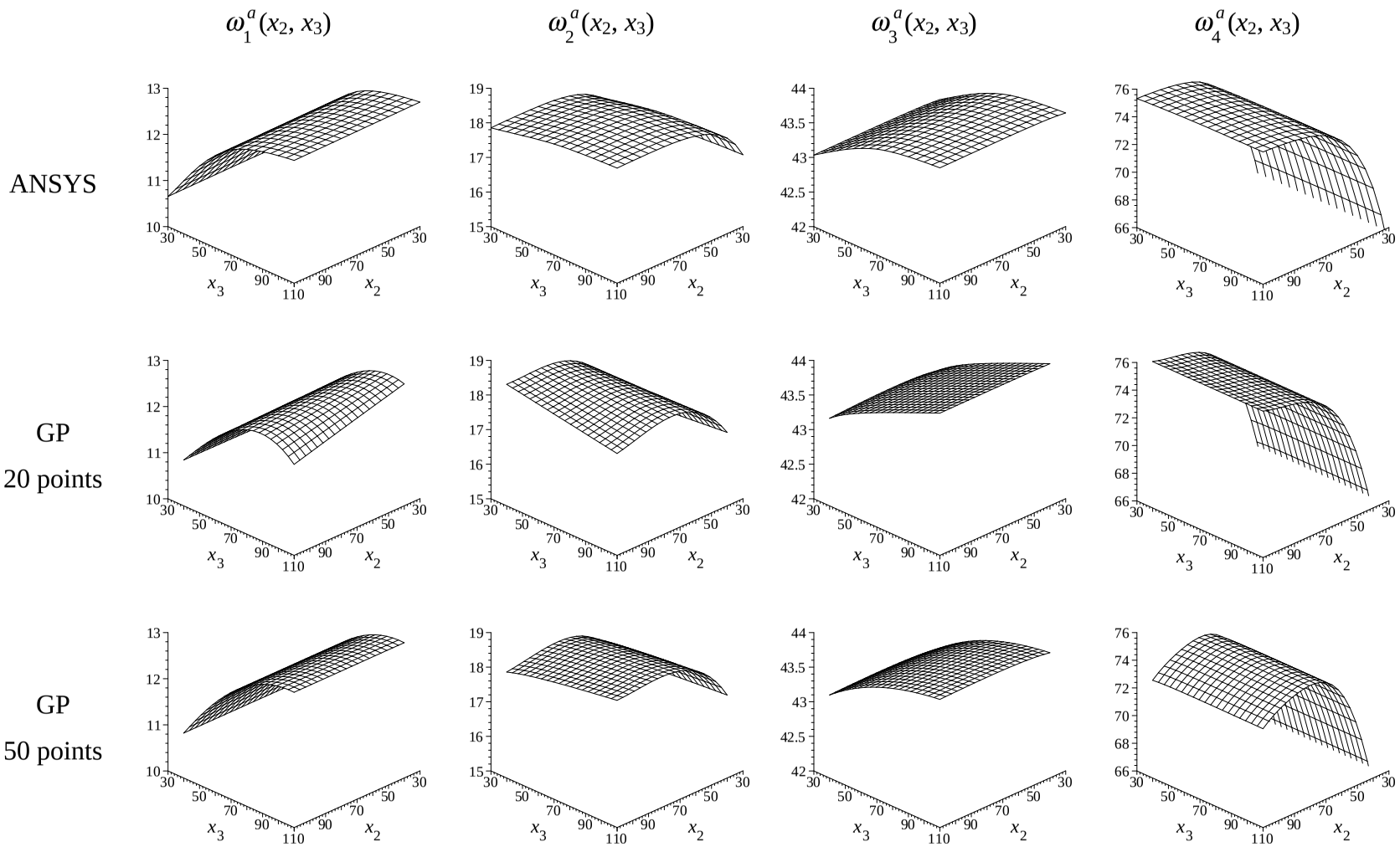

Figure 5.9 Approximation of individual frequencies $x_1 = 100$

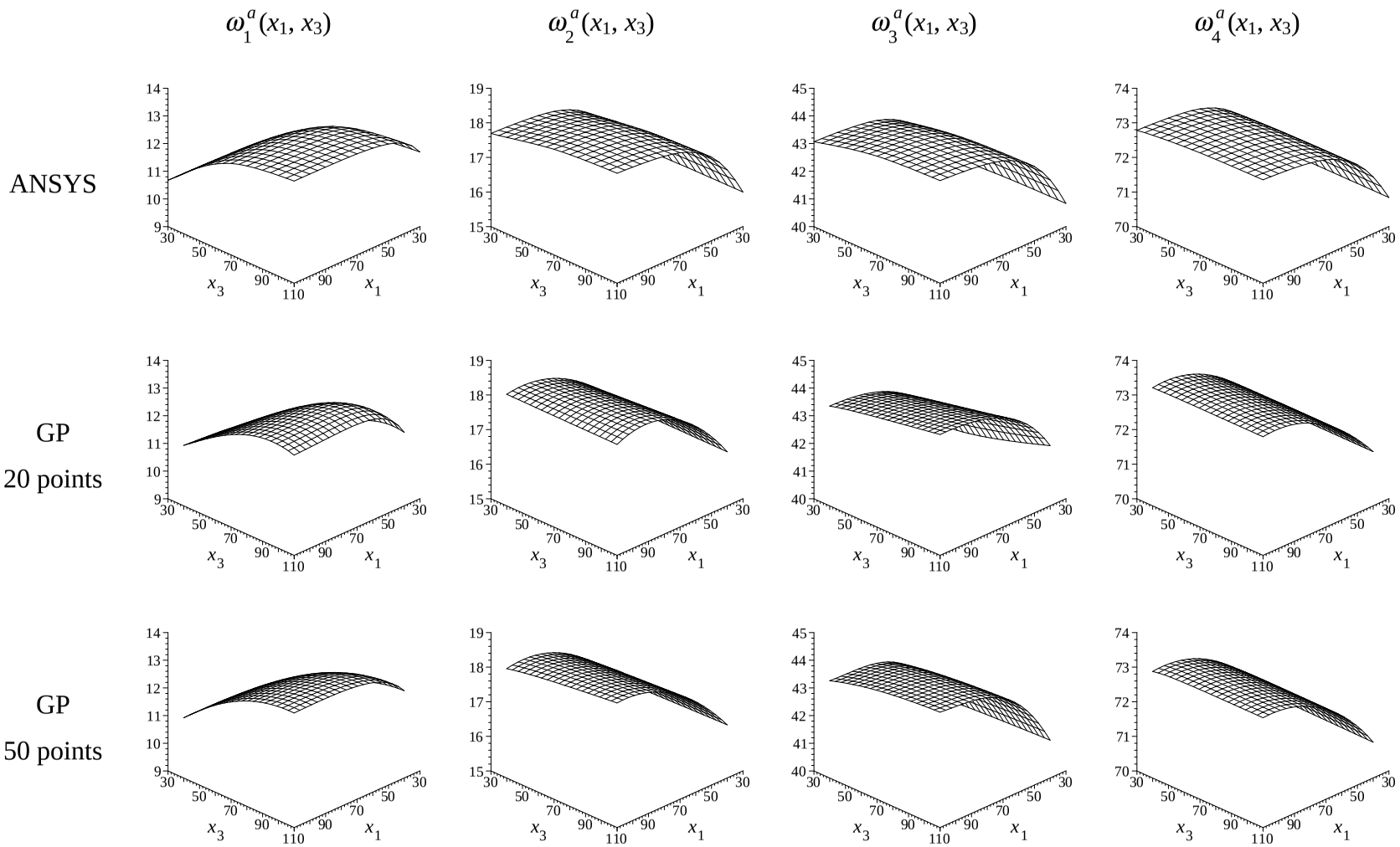

Figure 5.10 Approximation of individual frequencies $x_2 = 54$

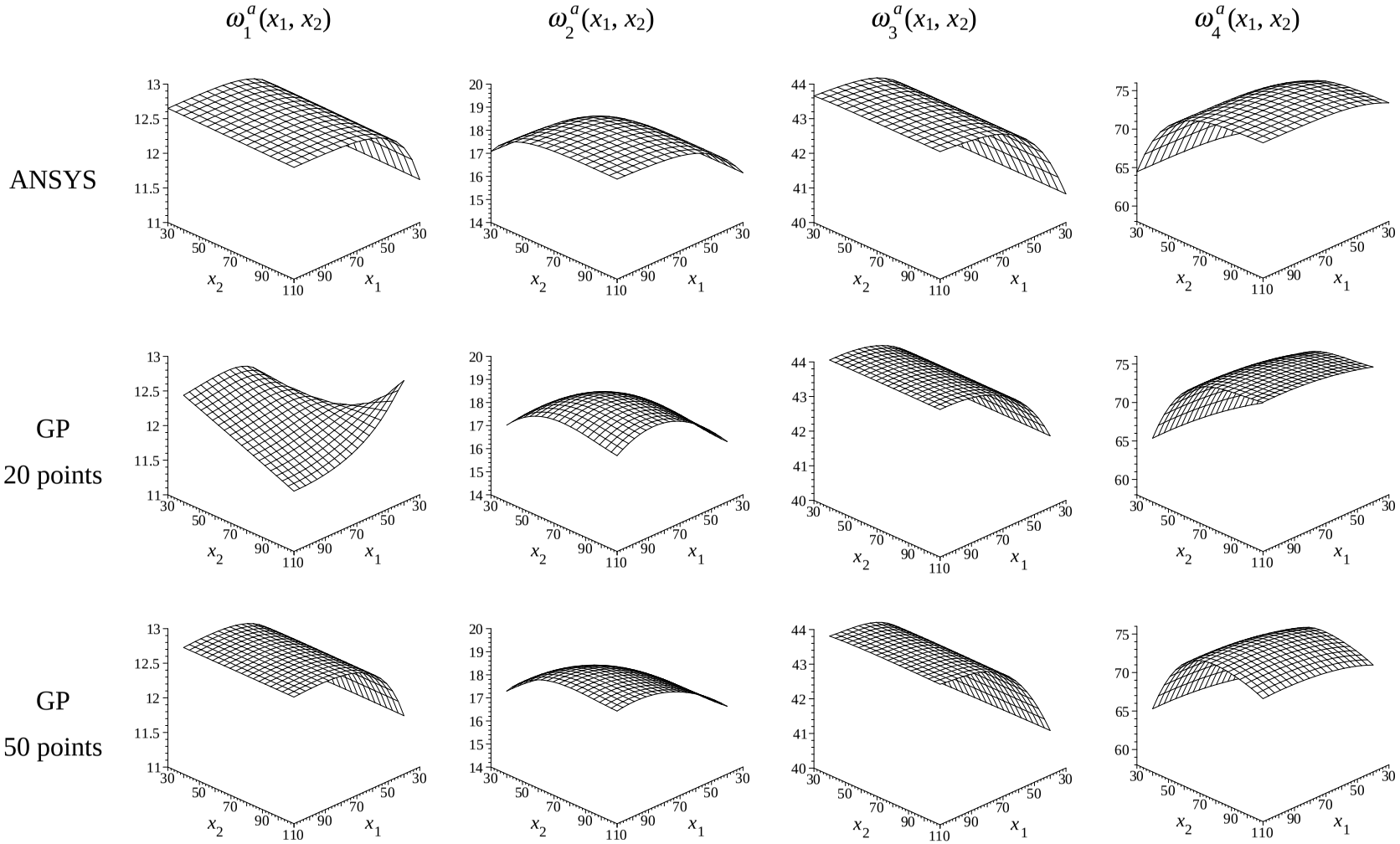

Figure 5.11 Approximation of individual frequencies $x_3 = 100$

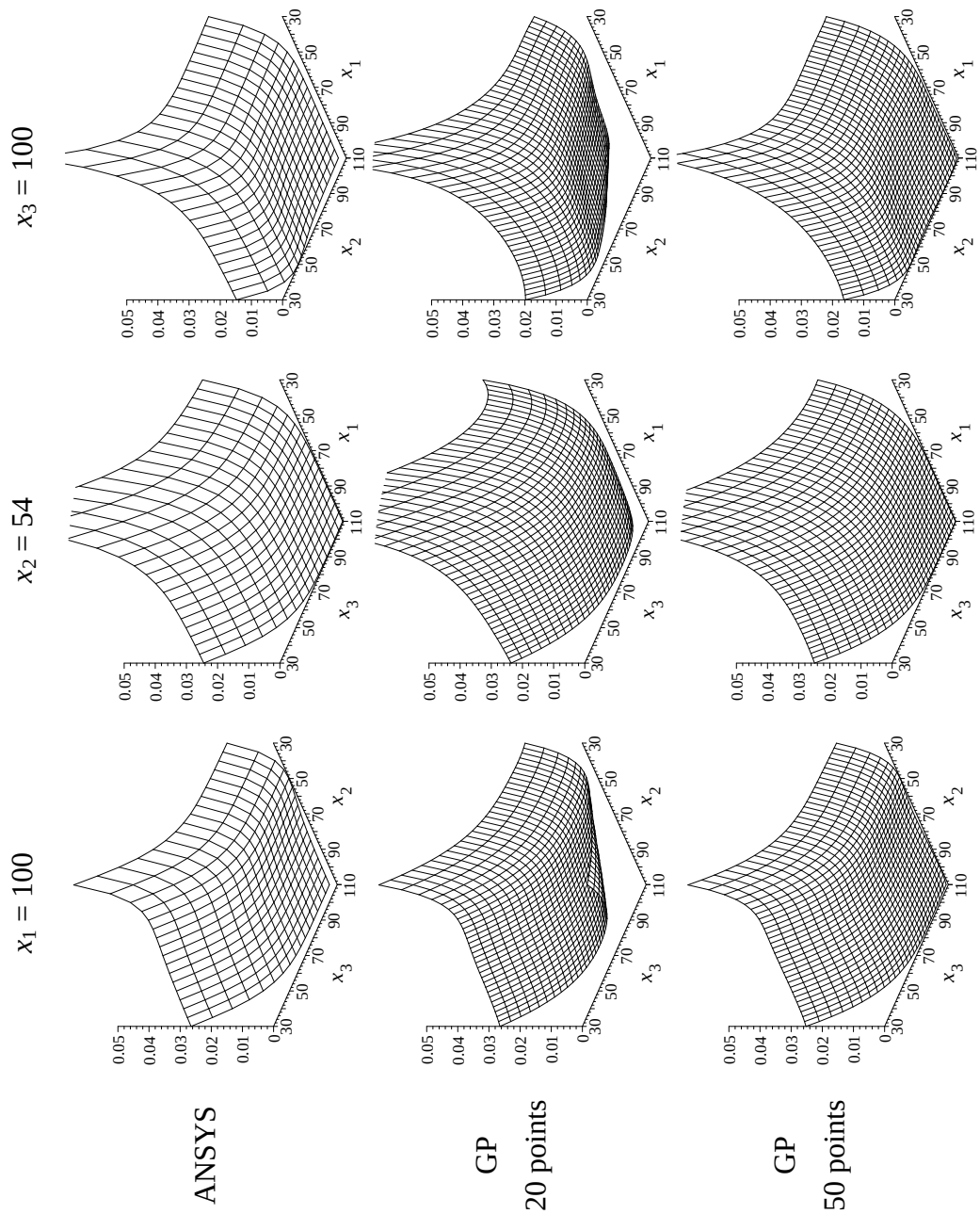

Figure 5.12 Approximation of individual frequencies: overall expression

The equations corresponding to all the approximations are described in Appendix A.

Both sets of the obtained results, corresponding to two alternative formulations of the approximation, allowed to recognise position of the damage as the value of x_2 is consistently smaller than the values of x_1 and x_3, thus indicating the presence of damage in the second location.

Interim results of this section have been reported in Toropov and Alvarez (1999a, 1999b) and Chapman et al. (1999).

5.6 Conclusion

GP has been successfully applied to problems with numerically simulated response. Two important aspects of RSM have been considered that confirm the following points:

- A larger number of points in the plan of experiments is desirable to obtain a better quality of the approximation (examples 5.1 and 5.4).
- The use of derivatives, if available, helps to reduce the necessary number of points necessary in the plan of experiments (example 5.3).

Example 5.4 has also demonstrated that GP is able to provide a solution even if a very large range of the optimization variables is adopted.

Interim results of this section have been reported in Toropov and Alvarez (1998b, 1998c, 1998d).